

Research Article

Open Access



# Tubular cubic polynomial sonotrode for green and sustainable ultrasonic welding technology

Khurram Hameed Mughal<sup>1,2</sup>, Salman Abubakar Bugvi<sup>1</sup>, Muhammad Fawad Jamil<sup>1,3</sup>, Muhammad Asif Mahmood Qureshi<sup>2</sup>, Fazal Ahmad Khalid<sup>4</sup>, Asif Ali Qaiser<sup>5</sup>

<sup>1</sup>Mechanical Engineering Department, The University of Lahore, Lahore 54000, Pakistan.

<sup>2</sup>Mechanical Engineering Department, University of Engineering and Technology, Lahore 54890, Pakistan.

<sup>3</sup>Department of Mechanical Engineering, Tsinghua University, Beijing 100084, China.

<sup>4</sup>Faculty of Materials and Chemical Engineering, GIK Institute of Engineering Sciences and Technology, Topi 23640, Pakistan.

<sup>5</sup>Polymer and Process Engineering Department, University of Engineering and Technology, Lahore 54890, Pakistan.

**Correspondence to:** Asst. Prof. Khurram Hameed Mughal, Mechanical Engineering Department, The University of Lahore, 1-km Defence Road, Lahore 54000, Pakistan. E-mail: khurram.hameed@me.uol.edu.pk

**How to cite this article:** Mughal KH, Bugvi SA, Jamil MF, Qureshi MAM, Khalid FA, Qaiser AA. Tubular cubic polynomial sonotrode for green and sustainable ultrasonic welding technology. *Green Manuf Open* 2023;1:14. <https://dx.doi.org/10.20517/gmo.2023.06>

**Received:** 30 Jun 2023 **First Decision:** 10 Aug 2023 **Revised:** 31 Aug 2023 **Accepted:** 22 Sep 2023 **Published:** 10 Oct 2023

**Academic Editors:** Lei Zhang, Hongchao Zhang **Copy Editor:** Dong-Li Li **Production Editor:** Dong-Li Li

## Abstract

Ultrasonic Welding has emerged as a sustainable, green, and efficient manufacturing technology. This technique joins unique and advanced materials quickly, with good welding quality through high-intensity vibrations. Ultrasonic welding uses relatively low energy and incurs lower costs compared to various conventional welding systems. One of the key aspects to ensure high welding quality and strength, along with the transmission of high forces, is the design of an efficient ultrasonic sonotrode. This research study is aimed at proposing, evaluating, and testing the design of a tubular cubic polynomial sonotrode using finite element analysis. This novel ultrasonic welding sonotrode operates with low stresses and high displacement amplification. The performance of the proposed ultrasonic welding sonotrode design was compared with the commercially popular sonotrode, as well as cubic Bezier, exponential, and conical designs. This comparison was done in terms of harmonic excitation response, stresses, axial stiffness, displacement amplification, and factor of safety. The performance characteristics were also evaluated along the sonotrode length. The proposed sonotrode was found to be superior in terms of high vibration amplification and axial stiffness within safe stress limits. The benefits of the flexible design as per requirement to attain a higher displacement amplitude at the output end; consequently, lower welding forces were also realized. The proposed design is an improvement towards an efficient and green manufacturing technology involving reduced cost, energy consumption, use of consumables, effort, waste generation, and harm to the environment.

**Keywords:** Cubic polynomial sonotrode design, finite element analysis, harmonic excitation response, ultrasonic welding, vibration amplification



© The Author(s) 2023. **Open Access** This article is licensed under a Creative Commons Attribution 4.0 International License (<https://creativecommons.org/licenses/by/4.0/>), which permits unrestricted use, sharing, adaptation, distribution and reproduction in any medium or format, for any purpose, even commercially, as long as you give appropriate credit to the original author(s) and the source, provide a link to the Creative Commons license, and indicate if changes were made.



## INTRODUCTION

Modern manufacturing has undergone major changes across the four industrial revolutions. These changes started with the use of steam engines and have been followed by the recent emergence of Industry 4.0 technologies such as additive manufacturing, three-dimensional (3D) printing, and mass customization in manufacturing. The focus has also shifted towards sustainability and the reduction in consumption. New smart materials having advanced manufacturing and process capabilities are being developed. The properties such as brittleness, ductility, strength-to-weight ratio, thermal insulation, heat dissipation, and operating life are being investigated for manufacturability. Ultrasonic welding has evolved as a new technology that has the ability to bond numerous materials efficiently and reliably, solving multiple problems in manufacturing. Ultrasonic welding works on the principle of generating vibrations that have high frequencies equal to or above 20 kHz and displacement amplitude of at least 5  $\mu\text{m}$ <sup>[1-7]</sup>.

Ultrasonic welding has a number of advantages, such as the ability to weld advanced materials quickly and efficiently at lower cost and using lower energy. It can realize the welding between similar and dissimilar materials such as metals, inorganic materials, and composite materials. It is a clean technology without any emission of sparks, dust, and fumes. It also involves minimal usage of consumables with less waste, making it an environmentally friendly, sustainable, and green manufacturing technique<sup>[1-3,5,6]</sup>. Ultrasonic welding of carbon fiber (CF)/PPS composites provided 15% higher lap shear strength (LSS) compared to resistance welding<sup>[8]</sup>. Ultrasonic welding of thermoplastic composites attained 3.83 % and 2.53 % higher LSS of welded joints compared to induction welding and resistance welding, respectively<sup>[9]</sup>. The electrochemical performance of injection-molded microfluidic chips bonded by ultrasonic welding was also found to be significantly superior compared to the ones obtained using thermal bonding<sup>[10]</sup>. Ultrasonic welding of CF-reinforced polyetheretherketone (CF/PEEK) composites realized 62.5% and 88.16% higher LSS compared to the induction and transmission laser welding techniques, respectively, indicating a longer operating life. Ultrasonic welding was found to be the most versatile process as it did not require any specific material properties<sup>[11]</sup>. The welding attributes realized through ultrasonic welding techniques include shorter welding time, lower temperatures, reduced welding forces, decreased material usage, longer tool life with little to no maintenance, reduced waste, and improved bonding strength, weld quality, and efficiency. The use and applications of ultrasonic welding technology are continuously evolving with the identification of improvements in tools, processes, and applications for sustainability<sup>[1,3,12]</sup>.

The working principle of ultrasonic welding is based on the high-frequency vibrations that are induced in sonotrodes through ultrasonic transducers and generators. The advanced materials are welded together at the desired surfaces using the effects of high-intensity vibrations and static pressure on the workpiece<sup>[13]</sup>. The basic components of the ultrasonic welding machine consist of generators, transducers, boosters, and sonotrodes [Figure 1]. The working of the generator results in the conversion of a low-frequency electrical input (50-60 Hz) to a higher-frequency output ( $\geq 20$  kHz). This high-frequency electrical output from the generator is passed on to the ultrasonic transducer, which converts it into the mechanical vibrations. However, the displacement amplitude at the transducer end is low and not sufficient for an effective welding operation. These mechanical vibrations are enhanced to the appropriate amplitude by an ultrasonic sonotrode. This sonotrode is placed at the output end of the ultrasonic welding system. A booster can be placed as an additional unit between the transducer and sonotrode to further enhance the displacement amplitude. Various research works highlighted the sonotrode as an important component of the ultrasonic welding system, which increases the vibration amplitude for the effective welding of advanced materials<sup>[4,13]</sup>.

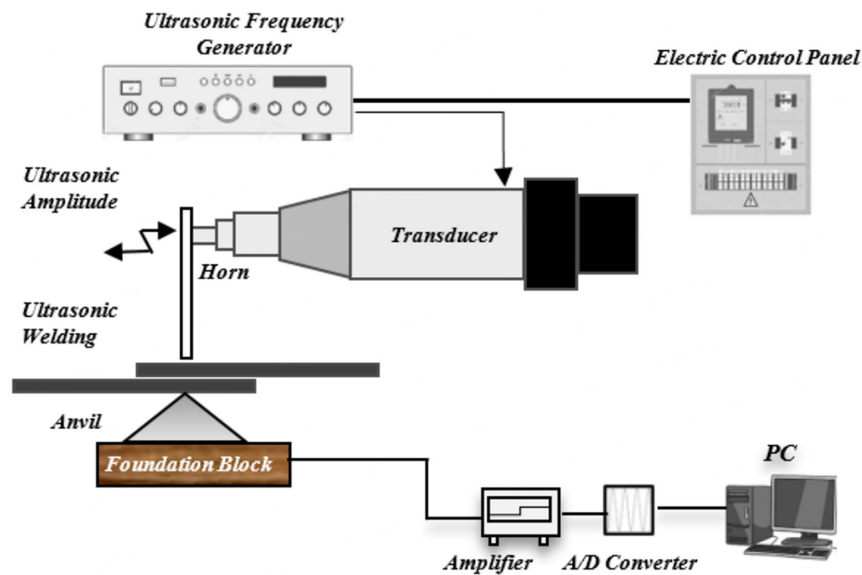


Figure 1. Ultrasonic welding system.

A number of studies have focused on the improvement of the design of an ultrasonic sonotrode, highlighting various profiles and methods for the performance improvement. Amin *et al.* studied the sonotrode design optimization with the inclusion of a cylindrical portion at the lower part of the sonotrode profile using finite element analysis (FEA)<sup>[14]</sup>. Wang *et al.* designed and developed a new sonotrode based on a cubic Bezier curve. They compared its performance with the stepped and the catenoidal sonotrodes in terms of stresses and magnification factors. They used the finite element method to design the sonotrode and incorporated a genetic algorithm for its optimization<sup>[12]</sup>. Nguyen *et al.* designed and optimized a non-rational B-spline (NURBS) sonotrode for the ultrasonic welding. The optimized NURBS sonotrode was found to have shape and displacement amplification closer to the stepped sonotrode. This particular sonotrode design did not provide significant improvement in the displacement amplification and the stress reduction compared to the stepped sonotrode, prompting limited usage in the ultrasonic welding<sup>[15]</sup>. Kumar *et al.* examined the design performance of the sonotrode with and without attachments to minimize the sonotrode failure and maximize the energy usage<sup>[6]</sup>. Wang *et al.* analyzed the stepped-type sonotrode for a specific ultrasonic welding application<sup>[16]</sup>. Razavi *et al.* analyzed a five-element sonotrode made of conical and cylindrical shapes using FEA<sup>[17]</sup>. Rai *et al.* evaluated the quadratic and cubic Bezier sonotrodes in terms of displacement amplification and stresses using FEA<sup>[18]</sup>. Mughal *et al.* designed a novel ultrasonic tool holder for the processing of advanced composites. Their tool design provided the greatest displacement amplification for a frequency ratio (ratio of the working frequency of a transducer to the natural frequency of a sonotrode) close to but less than one<sup>[19]</sup>. Mughal *et al.* analyzed a hollow Bezier ultrasonic tool holder to achieve high displacement amplification within the safe stress limits<sup>[20]</sup>. The effect of various geometric factors on the performance characteristics of the ultrasonic tool holder was studied by Mughal *et al.* in terms of stresses, modal frequencies, and displacement amplification<sup>[21,22]</sup>. Mughal *et al.* compared the performance of various ultrasonic sonotrode designs (such as Bezier, conical, catenoidal, exponential, and Gaussian, *etc.*) in terms of magnification factor, stresses, and modal frequencies<sup>[23-24]</sup>.

The investigations conducted by various researchers show the potential for developing new designs of ultrasonic sonotrodes for high displacement amplification and extended operating life. Out of the various designs, it has been noted that the stepped and the 3rd order Bezier sonotrodes have the ability to attain high displacement amplification and better welding attributes. The stepped sonotrode is liable for early

failure due to greater stress concentrations at the transition section. On the other hand, the Bezier sonotrode design is complex and requires a time-consuming optimization for achieving higher displacement amplification. It is desired to reduce the design complexity and optimization time and develop a solution for effective ultrasonic sonotrode design for good welding performance. During the study of the relevant literature, it was observed that the tubular cubic polynomial sonotrode profile for the ultrasonic welding application has never been tested for an axial modal frequency less than the transducer operating frequency ( $\omega_n < \omega$ ). The novelty of the manuscript pertains to the integration of the cubic polynomial sonotrode with a commercially available transducer to evaluate the harmonic excitation response of the ultrasonic welding tool for frequency ratios greater than one ( $\omega/\omega_n > 1$ ). It also proposes a method to enhance the vibration amplitude at the output end for the specified range of frequency ratios by removing the material to make it tubular, which also resulted in a lightweight structure and cost reduction. The demerits of the proposed sonotrode design pertain to the unavailability of the analytical solution and difficulty in precision manufacturing. Hence, the objective of this research was to design and propose an ultrasonic welding sonotrode to attain the greatest displacement amplification within safe stress limits for  $\omega/\omega_n > 1$ .

The finite element method was applied to compute the relevant modal frequency, displacement amplification, and stresses using the FEA software ANSYS. A comparative study of the displacement amplifications, stresses, and factors of safety among various sonotrode designs has been performed. The comparison provides robustness, reliability, and validity to the findings of the present research.

## METHODS

### Sonotrode designs

During ultrasonic welding, a high displacement amplification at the output end is an essential pre-requisite, along with reasonable stress levels and factors of safety. This is achieved through an efficient ultrasonic welding sonotrode design that is quite challenging and is dependent on the transducer and the required displacement amplification<sup>[4,12,13,16,19]</sup>.

Mughal *et al.* developed the generalized equation (1) for the sonotrode design that is dependent on the end diameters  $D_1$  &  $D_2$  and length  $L$ <sup>[19]</sup>. Figure 2A-D shows the commercially available sonotrode designs, which were compared with the proposed tubular cubic polynomial sonotrode [Figure 2E]. Their performance was analyzed for the frequency ratio greater than one using FEA. The sonotrode length was set to  $L = 114$  mm, with the rear and front-end diameters set to  $D_1 = 41$  mm and  $D_2 = 33$  mm, respectively, in accordance with the commercially popular ultrasonic welding tool. The working frequency of the ultrasonic tool was set at 20 kHz. Two designs were chosen after extensive numerical computations for tubular cubic polynomial sonotrodes based on the length ( $l$ ) and the diameter ( $d$ ) of the tubular section. For the novel cubic polynomial sonotrode-1,  $l$  and  $d$  were set equal to 57 and 15 mm, respectively. Whereas  $l$  and  $d$  were considered 30 and 15 mm, respectively, for the novel cubic polynomial sonotrode-2. Other designs include commercially popular stepped, conical, exponential, and cubic Bezier sonotrodes.

$$y = \frac{h}{2L^3}x^3 - \frac{3h}{2L^2}x^2 + \frac{D_1}{2} = \left(\frac{D_1 - D_2}{4L^3}\right)x^3 - \frac{3(D_1 - D_2)}{4L^2}x^2 + \frac{D_1}{2} \quad (1)$$

### Governing equations and finite element analysis

The governing equation of sonotrode response is given by Webster's equation (2)<sup>[4,19]</sup>.

$$\frac{\partial^2 u(x, t)}{\partial x^2} + \frac{\partial u(x, t)}{\partial x} \frac{\partial}{\partial x} \ln A(x) = \frac{1}{c^2} \frac{\partial^2 u(x, t)}{\partial t^2} \quad (2)$$

Where  $c = \sqrt{E/\rho}$  is the propagation velocity,  $u(x, t)$  is the axial displacement as a function of axial position “ $x$ ” and time “ $t$ ”,  $C_1$  &  $C_2$  are the parameters dependent on the initial conditions, and  $A(x)$  is the cross-sectional area. These stresses can be calculated using the governing equations 3-5 in the cylindrical coordinate system. The radial, axial, and tangential stresses are denoted by  $\sigma_r$ ,  $\sigma_\theta$ , and  $\sigma_z$ , while the shear stresses are denoted by  $\tau_{r\theta}$ ,  $\tau_{\theta z}$ , and  $\tau_{rz}$ , respectively. These stresses were utilized to calculate the principal stresses ( $\sigma_1, \sigma_2, \sigma_3$ ) and then von Mises stress  $\sigma_{VM}$ .

$$\frac{\partial \sigma_r}{\partial r} + \frac{1}{r} \frac{\partial \tau_{r\theta}}{\partial \theta} + \frac{\partial \tau_{rz}}{\partial z} + \frac{\sigma_r - \sigma_\theta}{r} = \rho \frac{\partial^2 u_r}{\partial t^2} \quad (3)$$

$$\frac{\partial \tau_{r\theta}}{\partial r} + \frac{1}{r} \frac{\partial \sigma_\theta}{\partial \theta} + \frac{\partial \tau_{\theta z}}{\partial z} + \frac{2\tau_{r\theta}}{r} = \rho \frac{\partial^2 u_\theta}{\partial t^2} \quad (4)$$

$$\frac{\partial \tau_{rz}}{\partial r} + \frac{1}{r} \frac{\partial \tau_{\theta z}}{\partial \theta} + \frac{\partial \sigma_z}{\partial z} + \frac{\tau_{rz}}{r} = \rho \frac{\partial^2 u_z}{\partial t^2} \quad (5)$$

$$\sigma_{VM} = \sqrt{[(\sigma_1 - \sigma_2)^2 + (\sigma_2 - \sigma_3)^2 + (\sigma_3 - \sigma_1)^2]/2} \quad (6)$$

Due to the ductile nature of the materials of ultrasonic welding sonotrodes, the factor of safety was determined by using the material’s yield strength  $\sigma_Y$  and maximum von Mises stress.

$$FS = \sigma_{VM}/\sigma_Y \quad (7)$$

The displacement amplification attained through ultrasonic welding sonotrodes was computed from the ratio of displacement amplitude at the sonotrode output end and the transducer output displacement<sup>[4,19]</sup>. Modal analysis was performed on various sonotrode materials to determine the resonant frequency under the given operating conditions and free oscillations. This was done in order to ensure the synchronization of the integrated assembly of the transducer and the sonotrode. The geometric parameters and the material properties of the sonotrode influence its resonant frequencies and associated parameters. The vibration modes of an engineering system include longitudinal, bending, torsional, or any combination of these. This ultrasonic system under consideration vibrates axially; therefore, the longitudinal mode of vibrations and accompanying frequency were taken into account. The frequency response function was examined to discover the resonant frequencies in the range of 0-40 kHz.

For the modal analysis, free vibrations of ultrasonic sonotrode are expressed in equation (8):

$$M\ddot{U} + C\dot{U} + KU = 0 \quad (8)$$

Where  $C$   $M$  and  $K$  are damping, mass, and stiffness matrices, and  $U$   $\dot{U}$  and  $\ddot{U}$  are displacement, velocity, and acceleration of the vibrating ultrasonic sonotrode. The damping of the ultrasonic sonotrode vibrating in the air can be considered negligible; therefore, the equation of motion representing free un-damped vibrations of ultrasonic sonotrodes can be written as:

$$M\ddot{U} + KU = 0 \quad (9)$$

The modal characteristics of an ultrasonic welding sonotrode are determined by solving equation (10), wherein the solution will be in terms of mode shapes (Eigenvectors,  $\varphi_i$ ) and associated modal frequencies (Eigenvalues,  $\omega_{n_i}$ ).

$$(K - \omega_{n_i}^2 M)\varphi_i = 0 \quad (10)$$

As illustrated in [Figure 2](#), the 3D geometry of the ultrasonic welding sonotrode was modeled using commercial CAD software (SolidWorks) and then transferred to the FEA software (ANSYS) for meshing and analysis. Tetrahedral elements were used to mesh the model because of their capability to model complicated and irregular geometries [[Figure 3](#)]. To get precise numerical results, a mesh independence analysis was performed<sup>[4,19-27]</sup>. The mesh element size was finalized to be 1 mm with 482,756 nodes and 283,397 elements because additional reductions in mesh size did not improve the results when the finite element model reached its convergence. Modal and harmonic analysis was performed as an integral aspect of the design process for ultrasonic welding sonotrodes to compute the modal frequencies, axial stiffness, displacement amplification, stresses, and factor of safety.

The fundamental goal of this study is to enable selective materials and sonotrode design to be used for green and sustainable ultrasonic welding technology and ensure a permanent process matching durable welding tools and good-strength junctions. The piezoelectric disc and rear and front metal plates of the commercial ultrasonic transducer and the sonotrode were used as the linearly elastic components. Aluminum alloy (AA 7075) and lead zirconate titanate material (PZT-5H) were utilized for the ultrasonic transducer metal blocks and transducer discs, with parameters reported in [Table 1](#)<sup>[4,12]</sup>. Steel (S) and stainless steel (SS) were used as the sonotrode materials. The performance of the proposed tubular cubic polynomial sonotrode was evaluated and compared with that of commercially popular stepped, cubic Bezier, exponential, and conical sonotrodes in terms of displacement amplification, axial stiffness, stresses, and factor of safety. The operating conditions, end diameters, and lengths for all the ultrasonic welding sonotrodes were considered the same for a better comparison. An electrical signal is provided to the ultrasonic transducer, which converts it to the mechanical vibrations. The harmonic excitation response analysis was carried out by considering the same displacement amplitude at the transducer end. [Figure 4](#) depicts a typical experimental setup for measuring the displacement amplification of an ultrasonic welding tool using a Laser Doppler Vibrometer LV1800 with LV-0112 displacement output boards and an electronic displacement meter LV-0121A.

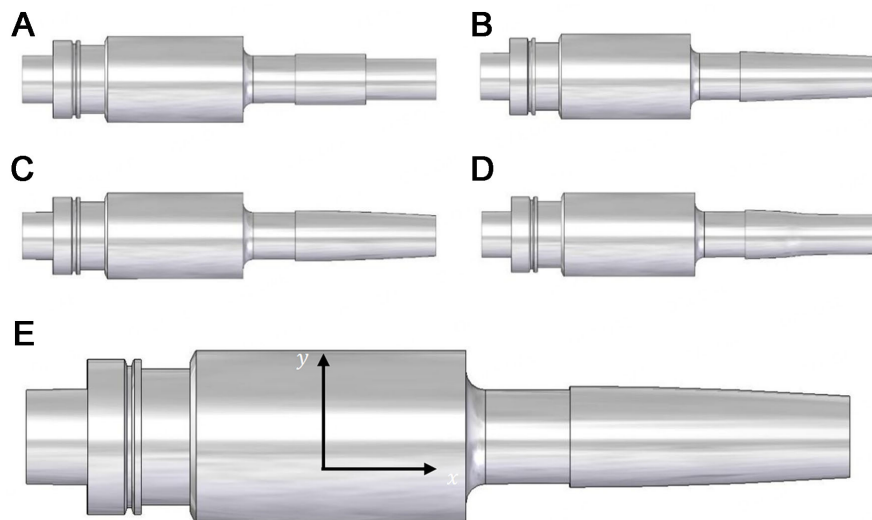
## RESULTS AND DISCUSSIONS

### Finite element simulation results

The steady-state harmonic excitation response of the ultrasonic welding tool in terms of the displacement amplification was determined using FEA. In [Figure 5](#), the displacement contour plot of the proposed ultrasonic welding sonotrode design has been presented. An input ultrasonic frequency was provided using a harmonic displacement on the input end of the sonotrode. The output end of the sonotrode was required to vibrate only in the axial direction for maximum energy utilization without any transverse movement. The maximum displacement amplification was attained at the output end of the proposed ultrasonic welding sonotrode with magnitude 8.44  $\mu\text{m}$ , validating the correctness of the research methodology used. This output end displacement causes an ultrasonic movement of the sonotrode tip, which creates an ultrasonic welding frictional effect between the mating components. A gradual and smooth increase in the displacement amplitude was observed throughout the length of the sonotrode.

**Table 1. Properties of the ultrasonic transducer and sonotrode materials**

Material	Properties	Value
PZT-5H	Piezoelectricity (C/m <sup>2</sup> )	$[d] = \begin{bmatrix} 0 & d_{12} & 0 \\ 0 & d_{22} & 0 \\ 0 & d_{12} & 0 \\ d_{41} & 0 & 0 \\ 0 & 0 & 0 \\ 0 & 0 & d_{66} \end{bmatrix} = \begin{bmatrix} 0 & -6.55 & 0 \\ 0 & 23.3 & 0 \\ 0 & -6.55 & 0 \\ 17.0 & 0 & 0 \\ 0 & 0 & 0 \\ 0 & 0 & 17.0 \end{bmatrix}$
	Permittivity (F/m)	$[\epsilon] = \begin{bmatrix} \epsilon_{11} & 0 & 0 \\ 0 & \epsilon_{22} & 0 \\ 0 & 0 & \epsilon_{33} \end{bmatrix} = 10^{-9} \times \begin{bmatrix} 15.052 & 0 & 0 \\ 0 & 13.015 & 0 \\ 0 & 0 & 15.052 \end{bmatrix}$
	Stiffness (N/m <sup>2</sup> )	$[c] = \begin{bmatrix} c_{11} & c_{12} & c_{13} & 0 & 0 & 0 \\ c_{21} & c_{22} & c_{23} & 0 & 0 & 0 \\ c_{31} & c_{32} & c_{33} & 0 & 0 & 0 \\ 0 & 0 & 0 & c_{44} & 0 & 0 \\ 0 & 0 & 0 & 0 & c_{55} & 0 \\ 0 & 0 & 0 & 0 & 0 & c_{66} \end{bmatrix} = 10^9 \times \begin{bmatrix} 127.2 & 84.7 & 80.2 & 0 & 0 & 0 \\ 84.7 & 117.4 & 84.7 & 0 & 0 & 0 \\ 80.2 & 84.7 & 127.2 & 0 & 0 & 0 \\ 0 & 0 & 0 & 23.0 & 0 & 0 \\ 0 & 0 & 0 & 0 & 23.5 & 0 \\ 0 & 0 & 0 & 0 & 0 & 23.0 \end{bmatrix}$
	Density (kg/m <sup>3</sup> )	7,600
High speed steel (S)	Elastic modulus (GPa)	71
	Poisson's ratio	0.33
	Density (kg/m <sup>3</sup> )	2,770
Stainless steel (SS)	Elastic modulus (GPa)	200
	Poisson's ratio	0.3
	Density (kg/m <sup>3</sup> )	7,850

**Figure 2.** Commercial ultrasonic transducer with (A) stepped (B) conical (C) exponential (D) cubic Bezier and (E) proposed tubular cubic polynomial sonotrodes.

The ultrasonic welding tool is a continuous system and has infinite vibration modes. Three basic vibration modes of ultrasonic welding tools are presented in Figure 6, which are the axial [Figure 6A], the bending [Figure 6B], and the torsional modes [Figure 6C]. All other modes are either advanced versions or combinations of these basic modes of vibrations. The bending and torsional vibrations of the sonotrode do not contribute effectively to the ultrasonic welding process. The ultrasonic transducer provides vibrations in

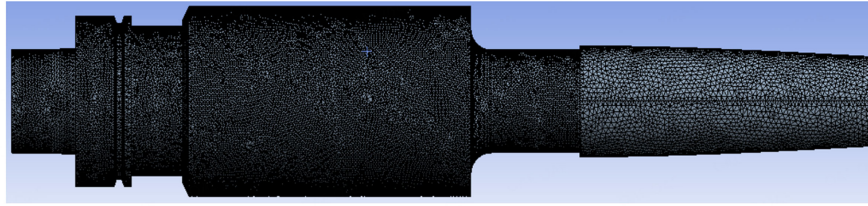


Figure 3. Meshed model of the proposed ultrasonic welding tool.

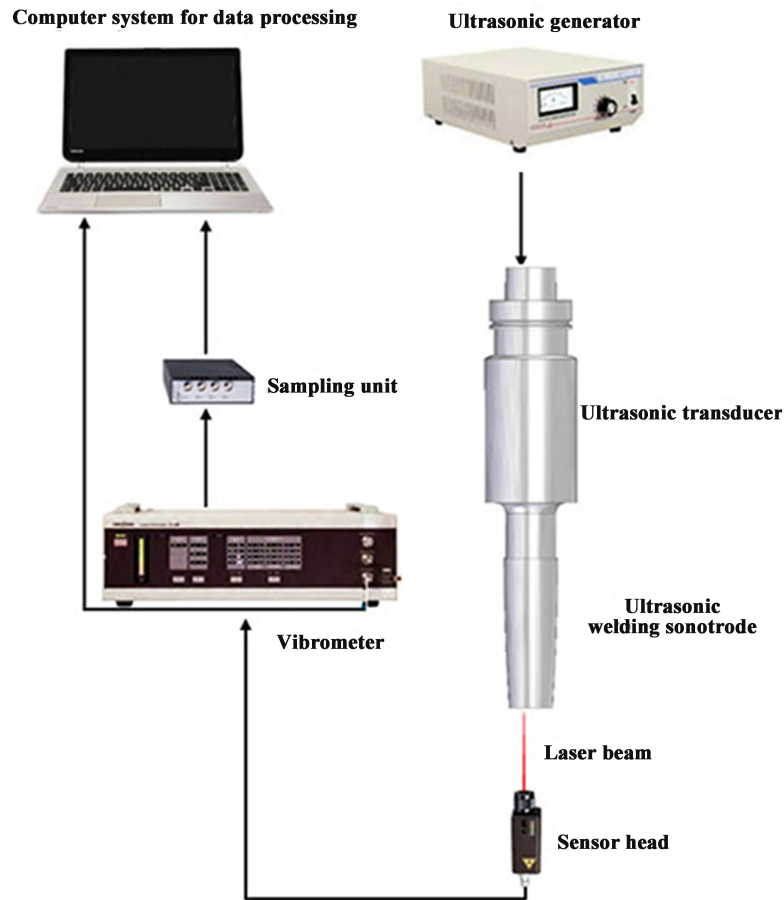


Figure 4. Experimental step for the measurement of the vibration characteristics of an ultrasonic welding tool.

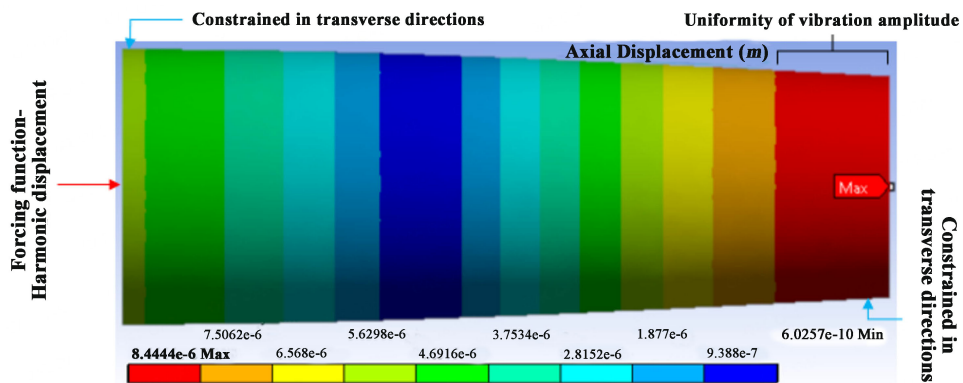
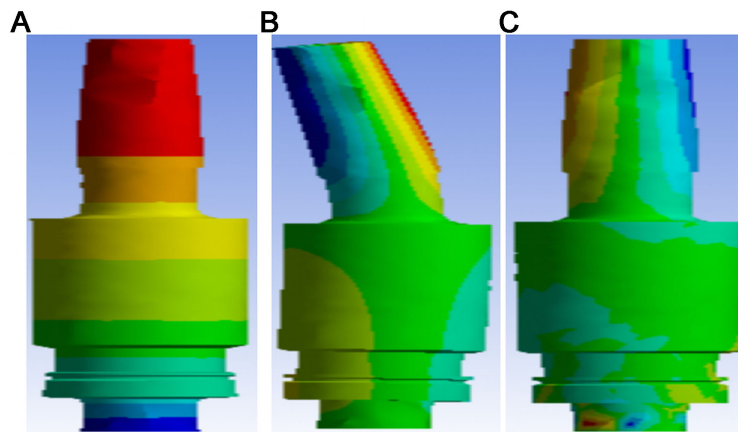


Figure 5. Displacement contour plot of ultrasonic welding sonotrode, along with boundary conditions.



**Figure 6.** Typical modes of ultrasonic tool vibrations: (A) Axial; (B) Bending; (C) Torsional.

the axial direction. Therefore, the axial mode of vibrations was searched and given preference to utilize the maximum amount of ultrasonic energy with minimum to no wastage. Additionally, no coupling of vibration modes was observed near the operating frequency of the ultrasonic welding tool. This was also validated through the frequency response function analysis of the proposed sonotrode.

Figure 7 shows a comparison between the axial stiffness of various ultrasonic welding sonotrodes under similar operating conditions. The axial stiffness of the proposed ultrasonic welding sonotrode design was found to be the greatest among all comparative sonotrode designs considered in the present work, such as cubic Bezier, stepped, exponential, and conical. This indicates that the proposed sonotrode has the capability of withstanding higher loads with the least deformation and will restore to its original position quickly when disturbed.

#### **Axial displacement along ultrasonic welding sonotrode**

The variation of axial displacement along the length for various ultrasonic welding sonotrode designs is presented in Figure 8. The ultrasonic frequency response amplitude provided by the transducer was set at  $5\ \mu\text{m}$  for all sonotrodes being tested. The axial displacement was decreased first to reach the nodal point (where axial displacement is zero) and then started to increase to reach the maximum value at the output end. It was determined that the maximum displacement was achieved by the proposed tubular cubic polynomial ultrasonic welding sonotrode, followed by the commercial stepped, cubic Bezier, exponential, and conical designs. This was attributed to the closeness of its axial modal frequency to the transducer operating frequency. The displacement amplification of the conical sonotrode was found to be the least due to its axial modal frequency being far away from the transducer operating frequency. The comparison of the displacement amplification attained by various sonotrodes for different grades of steel is presented in Figure 9 under similar operating conditions. The displacement amplification attained by the steel sonotrodes was found to be slightly greater than those made by the SS, mainly due to a relatively low elastic modulus of SS contributing towards the lower axial modal frequencies.

#### **Variation of stress in ultrasonic welding sonotrode**

Stress is a very important factor in predicting the failure and the operating life of the ultrasonic welding sonotrode. The variation of stress in the sonotrode design is dependent on its shape. The comparison of stresses in various ultrasonic sonotrodes for different grades of steel is presented in Figure 10. The stresses were found to be the greatest in the commercial stepped sonotrode due to an abrupt variation in the cross-sectional area. The stresses in the SS sonotrodes were found to be slightly less than those of the steel

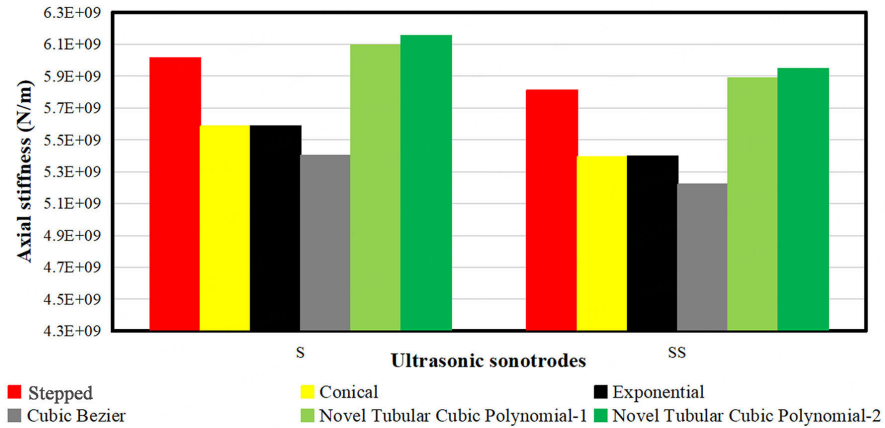


Figure 7. Comparison of axial stiffness for various ultrasonic welding sonotrodes.

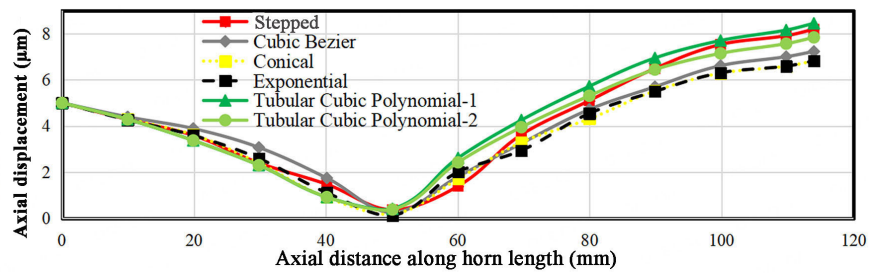


Figure 8. Variation of tool displacement along the length for various ultrasonic welding sonotrodes.

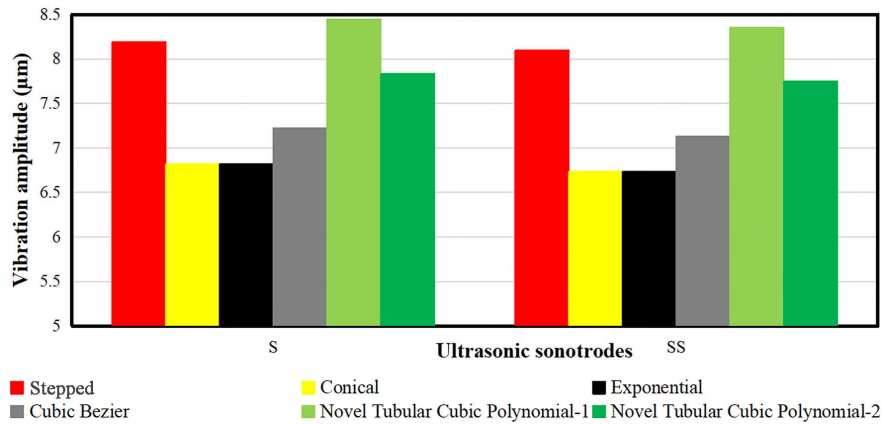


Figure 9. Comparison of vibration amplitude for various ultrasonic welding sonotrodes. S: Steel; SS: stainless steel.

sonotrodes due to the lower elastic modulus. The magnitudes of stress in the conical sonotrode were found to be the least among all ultrasonic sonotrodes considered in the present work.

Figure 11 presents the variation of von-Mises stresses along the length of various ultrasonic welding sonotrodes. High-stress concentrations in the stepped sonotrode at the transition section can easily be observed due to an abrupt variation in the cross-sectional area, which may cause early failure. This stress concentration can be avoided by incorporating a curve in the ultrasonic welding sonotrode design.

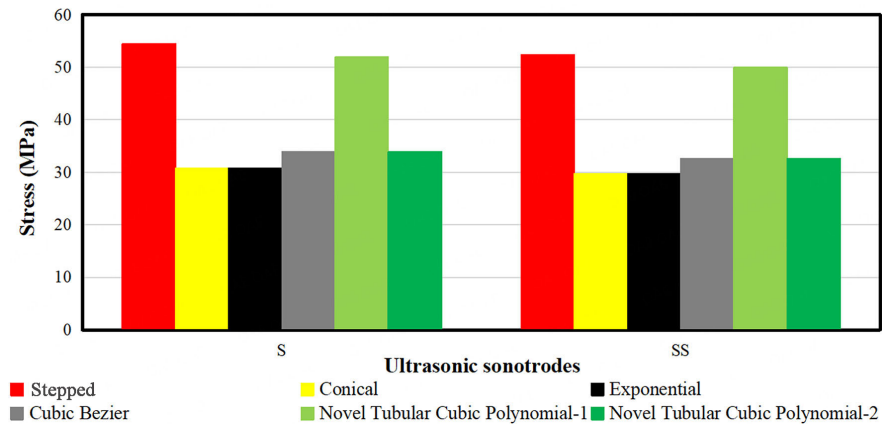


Figure 10. Comparison of stresses for various ultrasonic welding sonotrodes. S: Steel; SS: stainless steel.

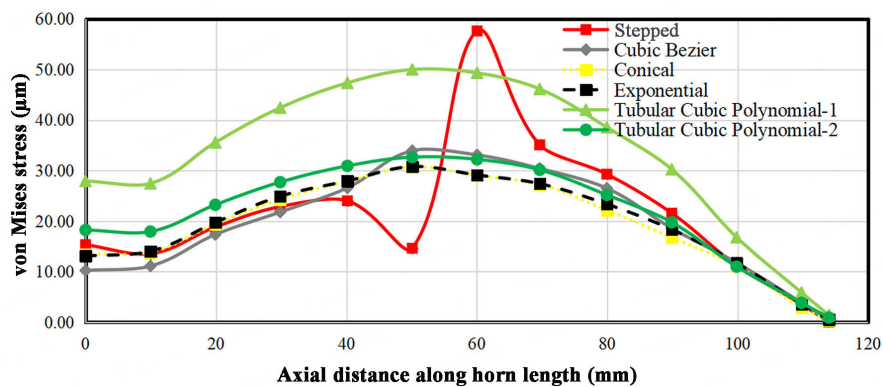
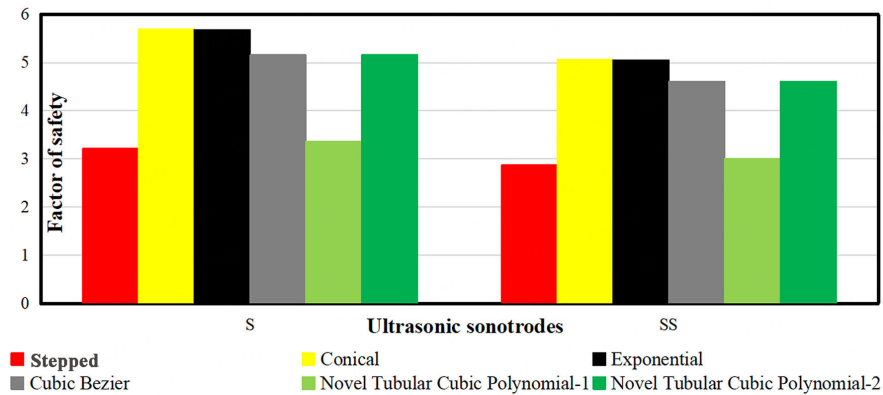


Figure 11. Variation of stresses along the length for various ultrasonic welding sonotrodes.

However, incorporating a curve can significantly reduce the vibration amplification as well. Therefore, a sonotrode design with the greatest vibration amplification but lower stresses than the commercial stepped design was essential for green and sustainable ultrasonic welding technology. This research fills this gap by proposing an ultrasonic welding sonotrode with the largest displacement amplification within safe stress limits for  $\omega/\omega_n > 1$ . A gradual and smooth increase in the displacement amplitude was observed throughout the sonotrode length compared to the commercially popular stepped sonotrode.

To predict the chances of failure and operating life of the ultrasonic welding sonotrode, the factor of safety was computed using the yield strength of the sonotrode material and the von Mises stress. The comparison of the safety factor for various ultrasonic sonotrodes is presented in Figure 12. The greatest factor of safety was attained by the conical design, while the commercially popular stepped sonotrode attained the least factor of safety. However, it is important to note that the displacement amplification achieved by the conical sonotrode is the least and much lower compared to the stepped design. Therefore, there is a tradeoff between the displacement amplification and the factor of safety for the design of the ultrasonic sonotrode. Hence, an optimum sonotrode design should be preferred for high displacement amplification and the factor of safety. The proposed ultrasonic welding sonotrode delivers greater vibration amplification with reasonable stress levels and factors of safety for  $\omega/\omega_n > 1$ .



**Figure 12.** Comparison of factors of safety for various ultrasonic welding sonotrodes. S: Steel; SS: stainless steel.

The large displacement amplification is beneficial for the efficient and high-quality ultrasonic welding of advanced materials; therefore, the proposed novel sonotrode [Figure 2E] with a commercial transducer was found to meet the design requirements of having good acoustic performance within safe working stress limits. Satpathy *et al.* worked on the sonotrode design for a high magnification and, thus, better acoustic performance<sup>[5]</sup>. A similar study by Amin *et al.* proposed an ultrasonic tool to have good acoustic performance in terms of high amplitude and low stress<sup>[14]</sup>. The proposed design of ultrasonic welding sonotrode provided high displacement amplification with low stress; therefore, it was found to meet the design requirements of having good acoustic performance within safe working stress limits. It was found suitable for the ultrasonic welding applications for advanced materials with performance better than the commercially popular stepped design and cubic Bezier sonotrode, along with the flexibility in performance. The achievement of a higher amplitude, with less design and manufacturing effort, would help enhance the welding attributes, i.e., bonding strength and welding quality and efficiency, that would result in minimalizing wastes and realizing an energy-efficient, clean, and sustainable environment. Finally, the low stresses in the proposed ultrasonic welding tool would cause a high factor of safety and, thus, longevity, which makes the proposed sonotrode a cost-effective design product.

## CONCLUSIONS

In this research work, the performance of a novel tubular cubic polynomial ultrasonic welding sonotrode was evaluated and compared with the other sonotrode designs for a frequency ratio greater than one. The harmonic excitation response was analyzed in terms of stress, displacement amplification, axial stiffness, and factor of safety under similar operating conditions using FEA. The main contribution of this research is the design of a low-cost and lightweight ultrasonic welding sonotrode with high vibration amplification within safe stress limits. It would cause reduced welding forces, time, interface temperature, consumption of energy, and material, along with enhanced bonding strength, welding quality, and efficiency. The dynamic performance of the proposed sonotrode was found to be exceptionally suitable to be used in green and sustainable ultrasonic welding technology.

For a high displacement amplification, low stresses, and better welding quality, the performance of the proposed ultrasonic sonotrode was found to be better than the commercially popular stepped, cubic Bezier, exponential, and conical sonotrodes. This is due to the closeness of its axial modal frequency with the operating frequency of the transducer. The axial stiffness of the proposed ultrasonic welding sonotrode was found to be the greatest, ensuring high resistance to applied loads and quick recovery after disturbance.

The stresses in the conical sonotrode were found to be the least with a high factor of safety; however, the amplification factor in the proposed design was found to be the greatest. The novel proposed design can be used where the transmission of high forces, pressures, and energy is required. The bonding strength and the weld quality typically improve as a result of enhanced vibration amplitude at the output end.

The future direction in which the research can be pursued includes the addition of helical slots to the suggested sonotrode design to boost its performance and create longitudinal-torsional coupled vibrations for improved ultrasonic welding attributes. The ultrasonic welding sonotrode may be vulnerable to a substantial rise in thermal and stress levels. This is a result of cyclic loading when used for extended periods of time with high vibration amplitudes. Future research might look at the temperature and endurance characteristics of the proposed ultrasonic welding sonotrodes.

## DECLARATIONS

### Authors' contributions

Writing-original draft, conceptualization, methodology, data analysis, data acquisition, interpretation and validation, and technical support: Mughal KH

Writing-original draft: Bugvi SA, Jamil MF

Technical support, supervision: Qureshi MAM, Khalid FA, Qaiser AA

### Availability of data and materials

Data can be made available upon request.

### Financial support and sponsorship

None.

### Conflicts of interest

All authors declared that there are no conflicts of interest.

### Ethical approval and consent to participate

Not applicable.

### Consent for publication

Not applicable.

### Copyright

© The Author(s) 2023.

## REFERENCES

1. Li H, Chen C, Yi R, Li Y, Wu J. Ultrasonic welding of fiber-reinforced thermoplastic composites: a review. *Int J Adv Manuf Technol* 2022;120:29-57. [DOI](#)
2. Lin J, Lin S. Study on a large-scale three-dimensional ultrasonic plastic welding vibration system based on a quasi-periodic phononic crystal structure. *Crystals* 2020;10:21. [DOI](#)
3. Zhao T, Zhao Q, Wu W, et al. Enhancing weld attributes in ultrasonic spot welding of carbon fibre-reinforced thermoplastic composites: effect of sonotrode configurations and process control. *Compos B Eng* 2021;211:108648. [DOI](#)
4. Mughal KH, Ahmad N, Hayat N, et al. Design and performance evaluation of a novel ultrasonic welding sonotrode for langevin transducer using finite element approach. *Int J Ind Eng Theory Appl Pract* 2023;30:971-85. [DOI](#)
5. Satpathy MP, Sahoo SK, Datta S. Acoustic horn design and effects of process parameters on properties of dissimilar ultrasonic welding aluminum to brass. *Mater Manuf Process* 2016;31:283-90. [DOI](#)
6. Kumar S, Ding W, Sun Z, Wu CS. Analysis of the dynamic performance of a complex ultrasonic horn for application in friction stir welding. *Int J Adv Manuf Technol* 2018;97:1269-84. [DOI](#)

7. Jongbloed B, Teuwen J, Benedictus R, Villegas IF. On differences and similarities between static and continuous ultrasonic welding of thermoplastic composites. *Compos B Eng* 2020;203:108466. DOI
8. Villegas IF, Moser L, Yousefpour A, Mitschang P, Bersee HE. Process and performance evaluation of ultrasonic, induction and resistance welding of advanced thermoplastic composites. *J Thermoplast Compos Mater* 2013;26:1007-24. DOI
9. O'shaughnessy P, Dubé M, Fernandez Villegas I. Modeling and experimental investigation of induction welding of thermoplastic composites and comparison with other welding processes. *J Compos Mater* 2016;50:2895-910. DOI
10. Korycki A, Garnier C, Bonmatin M, Laurent E, Chabert F. Assembling of carbon fibre/PEEK composites: comparison of ultrasonic, induction, and transmission laser welding. *Materials* 2022;15:6365. DOI PubMed PMC
11. Matteucci M, Heiskanen A, Zór K, Emnéus J, Taboryski R. Comparison of ultrasonic welding and thermal bonding for the integration of thin film metal electrodes in injection molded polymeric lab-on-chip systems for electrochemistry. *Sensors* 2016;16:1795. DOI PubMed PMC
12. Wang DA, Chuang WY, Hsu K, Pham HT. Design of a Bézier-profile horn for high displacement amplification. *Ultrasonics* 2011;51:148-56. DOI PubMed
13. Rani M, Rudramoorthy R. Computational modeling and experimental studies of the dynamic performance of ultrasonic horn profiles used in plastic welding. *Ultrasonics* 2013;53:763-72. DOI PubMed
14. Amin S, Ahmed M, Youssef H. Computer-aided design of acoustic horns for ultrasonic machining using finite-element analysis. *J Mater Process Technol* 1995;55:254-60. DOI
15. Nguyen HT, Nguyen HD, Uan JY, Wang DA. A nonrational B-spline profiled horn with high displacement amplification for ultrasonic welding. *Ultrasonics* 2014;54:2063-71. DOI PubMed
16. Wang J, Sun Q, Teng J, Jin P, Zhang T, Feng J. Enhanced arc-acoustic interaction by stepped-plate radiator in ultrasonic wave-assisted GTAW. *J Mater Process Technol* 2018;262:19-31. DOI
17. Razavi H, Keymanesh M, Golpayegani IF. Analysis of free and forced vibrations of ultrasonic vibrating tools, case study: ultrasonic assisted surface rolling process. *Int J Adv Manuf Technol* 2019;103:2725-37. DOI
18. Rai PK, Yadava V, Patel RK. Design of Bezier profile horns by using optimization for high amplification. *J Braz Soc Mech Sci Eng* 2020;42:309. DOI
19. Mughal KH, Qureshi MAM, Raza SF. Novel ultrasonic horn design for machining advanced brittle composites: a step forward towards green and sustainable manufacturing. *Environ Technol Innov* 2021;23:101652. DOI
20. Mughal KH, Qureshi MAM, Qaiser AA, et al. Tubular bezier horn optimum design for ultrasonic vibration assisted machining of nomex composite. In: 2022 19th International Bhurban Conference on Applied Sciences and Technology (IBCAST); 2022 Aug 16-20; Islamabad, Pakistan. IEEE; 2022. p. 26-32. DOI
21. Mughal KH, Qureshi MAM, Qaiser AA, et al. Numerical investigation of the effect of uniform cutout on performance of ultrasonic horn for machining nomex honeycomb core material. *Jurnal Kejuruteraan* 2022;34:523-33. DOI
22. Mughal KH, Qureshi MAM, Hayat M, et al. Dynamic performance evaluation of ultrasonic composite horn for machining soft and brittle composites. *Jurnal Kejuruteraan* 2023;35:169-78. DOI
23. Mughal KH, Qureshi MAM, Khalid FA, Qaiser AA. Harmonic excitation response of standard ultrasonic horn designs for machining nomex honeycomb core composite. *Jurnal Kejuruteraan* 2024;36:(in press).
24. KH, Qureshi MAM, Qaiser AA, Khalid FA. Numerical evaluation of state of the art horn designs for rotary ultrasonic vibration assisted machining of nomex honeycomb composite. *Technology* 2021;5:7-9. DOI
25. Mughal KH, Bugvi SA, Jamil MF, et al. Enhancement of aerodynamic performance of high-speed train through nose profile design: a computational fluid dynamics approach. *Jurnal Kejuruteraan* 2022;34:1237-50. DOI
26. Mughal KH, Bugvi SA, Qureshi MAM, Khan MA, Hayat K. Numerical evaluation of contemporary excavator bucket designs using finite element analysis. *Jurnal Kejuruteraan* 2021;33:579-91. DOI
27. Munir MM, Mughal KH, Qureshi MAM, Khalid FA, Qaiser AA. Design of novel longitudinally-torsionally coupled ultrasonic Bezier horns for machining advanced hard and brittle materials. *J Vib Eng Technol* 2023;(in press).